Archives of Biochemistry and Biophysics 494 (2010) 216–225

Contents lists available at ScienceDirect

Archives of Biochemistry and Biophysics

journal homepage: www.elsevier.com/locate/yabbi

Assembly of the Sos1–Grb2–Gab1 ternary signaling complex is under allosteric control

Caleb B. McDonald, Kenneth L. Seldeen, Brian J. Deegan, Vikas Bhat, Amjad Farooq *

Department of Biochemistry & Molecular Biology and USylvester Braman Family Breast Cancer Institute, Leonard Miller School of Medicine, University of Miami, Miami, FL 33136, United States

ARTICLE INFO

Article history:
Received 27 October 2009
and in revised form 7 December 2009
Available online 22 December 2009

Keywords:
Sos1–Grb2–Gab1 ternary signaling complex
SH3-ligand thermodynamics
Allosteric regulation
Isothermal titration calorimetry
Circular dichroism
Macromolecular modeling

ABSTRACT

Allostery has evolved as a form of local communication between interacting protein partners allowing them to quickly sense changes in their immediate vicinity in response to external cues. Herein, using isothermal titration calorimetry (ITC) in conjunction with circular dichroism (CD) and macromolecular modeling (MM), we show that the binding of Grb2 adaptor—a key signaling molecule involved in the activation of Ras GTPase—to its downstream partners Sos1 guanine nucleotide exchange factor and Gab1 docker is under tight allosteric regulation. Specifically, our findings reveal that the binding of one molecule of Sos1 to the nSH3 domain allosterically induces a conformational change within Grb2 such that the loading of a second molecule of Sos1 onto the cSH3 domain is blocked and, in so doing, allows Gab1 access to the cSH3 domain in an exclusively non-competitive manner to generate the Sos1–Grb2–Gab1 ternary signaling complex.

Introduction

Proteins are neither rigid bodies nor they act like nuts and bolts to execute their biological functions. In what has come to be known as allostery, proteins have evolved to become highly flexible molecules in a manner akin to the very living bodies that they energize. The notion that protein function requires motion is as old as the determination of maiden structure of a protein at atomic level in 1958 by Kendrew and co-workers [1], whereby it became immediately clear that the static structure of myoglobin contained no obvious route to allow the entry of an oxygen molecule to a virtually buried heme moiety at the center of the protein. Fast-forward to more than half a century later and our understanding of such allosteric binding of ligands to proteins remains largely elusive and, in particular, continues to be under-appreciated. Although originally perceived as a change in protein structure upon the binding of a small ligand, usually at a site remote from its functionally active or binding site, as embodied in the classical MWC model first put forward in the 1960s [2,3], what constitutes allostery does not necessarily have to be restricted to such a classical definition. The prevailing school of thought is that any change in protein structure or motion, local or global, in response to the binding of another molecule, be it a small molecule or another protein partner, falls within the bounds of allosteric behavior [4]. In an effort to further our understanding of the role of allostery in driving cellular processes, we embarked on the challenge of deciphering the molecular determinants of the binding of Grb2 adaptor to its downstream partners Sos1 and Gab1 as encountered in a multitude of signaling cascades that initiate at the cell surface and reach their climax in the nucleus. The modular design of Grb2, comprised of the ubiquitous nSH3–SH2–cSH3 signaling module where the nSH3 and cSH3 are the N-terminal and the C-terminal SH3 domains flanking the central SH2 domain, exquisitely befits its role as a key component of signaling networks involved in the transmission of chemical information from activated receptor tyrosine kinases (RTKs)[1] at the cell surface to downstream cytosolic targets such as Ras and Akt—effector molecules responsible for orchestrating a diverse array of cellular processes central to health and disease [5–8]. While Grb2 recognizes RTKs, such as EGFR, FGFR and PDGFR, by virtue of its SH2 domain to bind to tyrosine-phosphorylated (pY) sequences in the context of pYXN motif located within the cytoplasmic tails [9–11], the SH3 domains present an opportunity for a wide spectrum of proline-rich proteins to be recruited to the inner membrane surface—the site of initiation of a plethora of signaling cascades [7,12–19]. Among them, the Sos1 guanine nucleotide exchange factor and the Gab1 docker are by

* Corresponding author. Fax: +1 305 243 3955.
E-mail address: amjad@farooqlab.net (A. Farooq).

[1] *Abbreviations used:* CD, circular dichroism; EGFR, epidermal growth factor receptor; FGFR, fibroblast growth factor receptor; Gab1, Grb2-associated binder 1; Grb2, growth factor receptor binder 2; ITC, isothermal titration calorimetry; MAPK, mitogen-activated protein kinase; MM, macromolecular modeling; NMR, nuclear magnetic resonance; PDGF, platelet-derived growth factor receptor; RTK, receptor tyrosine kinase; SH2, Src homology 2; SH3, Src homology 3; Sos1, son of sevenless 1; Trx, thioredoxin; UV, ultra-violet.

0003-9861/$ - see front matter © 2009 Elsevier Inc. All rights reserved.
doi:10.1016/j.abb.2009.12.011

far the best characterized downstream partners of Grb2 [7,12–14]. Upon recruitment to the inner membrane surface, Sos1 facilitates the GDP–GTP exchange within the membrane-bound Ras GTPase and thereby switches on a key signaling circuit that involves the activation of MAP kinase cascade central to cellular growth and proliferation [20]. In contrast, the recruitment of Gab1 to the inner membrane surface provides docking platforms for the Shp2 tyrosine phosphatase and the PI3K lipid kinase, which respectively account for further amplification of Ras activity—as sustained activation of Ras requires both the Sos1-dependent and Gab1-dependent pathways [21–23]—and the activation of Akt serine-threonine kinase, which plays a pivotal role in cell growth and survival [24]. Despite the discovery of Grb2 nearly two decades ago [7–10], the precise mechanism by which Grb2 recruits Sos1 and Gab1 remains hitherto unresolved. The prevailing school of thought is that while both the nSH3 and cSH3 domains are required for the recruitment of Sos1, only the latter is necessary for Gab1 [14,25–29]. If this scenario were indeed to play out within the milieu of the cell, one would expect Sos1 and Gab1 to compete for Grb2 and thereby leading to the buildup of distinct Grb2–Sos1 and Grb2–Gab1 pools. This plausible scenario was however cut short by the demonstration that Sos1 and Gab1 do not compete for Grb2 but rather associate in a mutually inclusive manner leading to the formation of the Sos1–Grb2–Gab1 ternary signaling complex [30]. In an attempt to rationalize the assembly of this signaling complex, we hypothesized that the binding of one molecule of Sos1 to the nSH3 domain allosterically induces a conformational change within Grb2 such that the loading of a second molecule of Sos1 onto the cSH3 domain is blocked and, in so doing, allowing Gab1 access to the cSH3 domain in an exclusively non-competitive manner to generate the Sos1–Grb2–Gab1 ternary complex (Fig. 1a). Herein, using isothermal titration calorimetry (ITC) in conjunction with circular dichroism (CD) and macromolecular modeling (MM), we provide experimental evidence in support of this hypothesis. Taken together, our study adds to the notion that the perception of signaling proteins as "plug-and-play" devices is highly oversimplified and that allostery is the key to unlocking the complexity of cellular signaling cascades central to health and disease.

Materials and methods

Protein preparation

Full-length human Grb2 (residues 1–217) and the truncated construct Grb2_ΔSH2 (residues 1–60 & 151–217) in which the central SH2 domain was excised out and the two terminal SH3 domains were fused together were cloned into pET102 bacterial

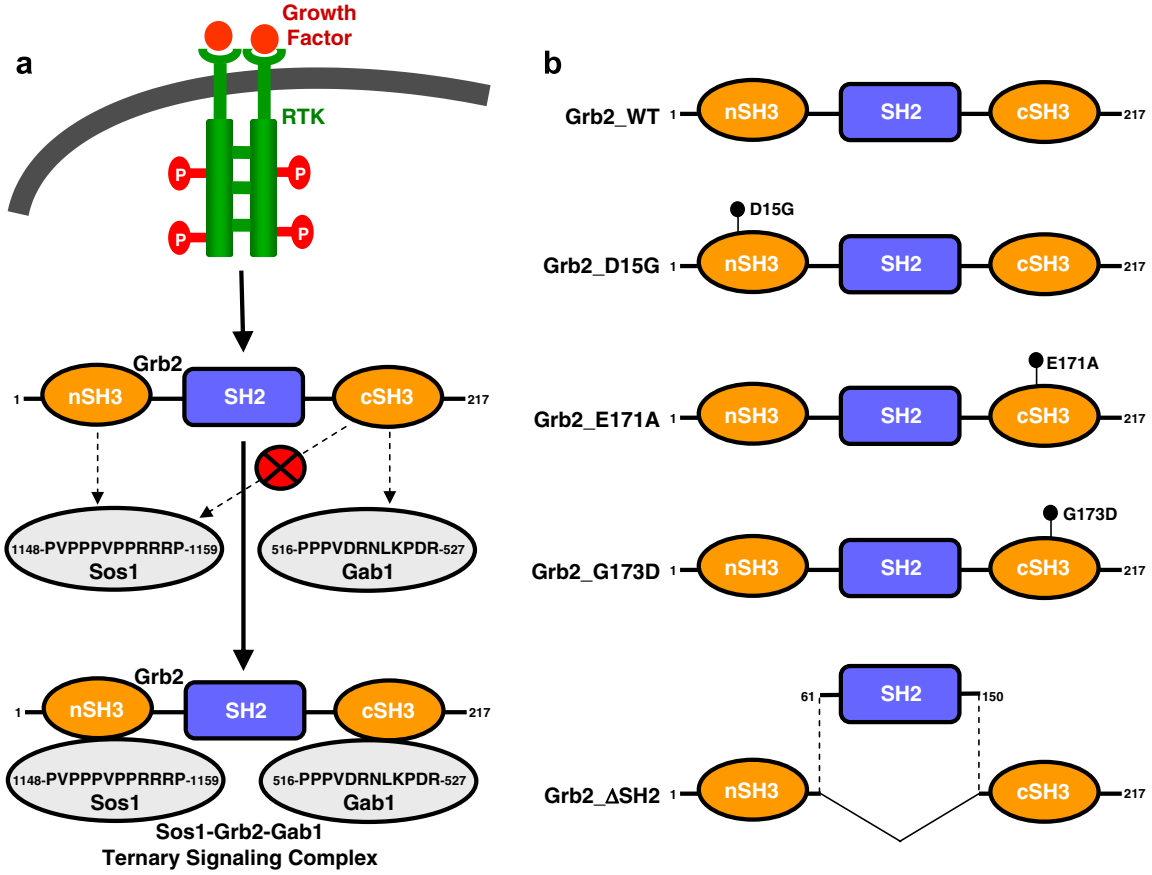

Fig. 1. Role of Grb2 in cellular signaling. (a) A schematic showing the assembly of Sos1–Grb2–Gab1 ternary signaling complex. Upon receptor stimulation, Grb2 is recruited to the inner membrane surface via the binding of its SH2 domain to tyrosine-phosphorylated (pY) sequences in the context of pYXN motif located within the cytoplasmic tails. The SH3 domains in turn recruit Sos1 and Gab1 as indicated in a mutually inclusive manner to generate the Sos1–Grb2–Gab1 ternary complex. Although the isolated cSH3 domain can bind to both Sos1 and Gab1, allosteric communication between the SH3 domains of Grb2 ensures that Sos1 solely binds to the nSH3 domain and thereby handing the cSH3 domain exclusive right to bind to Gab1. Note that the amino acid sequences of Sos1 and Gab1 shown correspond to respective peptides employed in this study. (b) Illustration of various Grb2 constructs used in this study. These include the wildtype Grb2 (Grb2_WT), D15G mutant of Grb2 (Grb2_D15G), E171A mutant of Grb2 (Grb2_E171A), G173D mutant of Grb2 (Grb2_G173D) and the truncated construct of Grb2 in which the central SH2 domain was excised out and the terminal SH3 domains were stitched together (Grb2_ΔSH2). Note that the D15G mutation abolishes the binding of nSH3 domain to Sos1, E171A mutation abolishes the binding of cSH3 domain to Sos1, and the G173D mutation renders the cSH3 domain into nSH3-mimetic in that it binds to Sos1 with comparable energetics to that observed for the binding of nSH3 domain [28].

expression vector with an N-terminal thioredoxin (Trx)-tag and a C-terminal polyhistidine (His)-tag using Invitrogen TOPO technology (Fig. 1b). Additionally, thrombin protease sites were introduced at both the N- and C-termini of the proteins to aid in the removal of tags after purification. Proteins were subsequently expressed in *Escherichia coli* Rosetta2(DE3) bacterial strain (Novagen) cultured in LB media and purified on a Ni–NTA affinity column as described previously [31]. Briefly, treatment of Ni–NTA elution fractions on a Hiload Superdex 200 size-exclusion chromatography (SEC) column interfaced to GE Akta FPLC system led to purification of recombinant proteins to apparent homogeneity as judged by SDS–PAGE analysis. The identity of recombinant proteins was further confirmed by MALDI-TOF mass spectrometry analysis. Protein yield was typically between 20 and 30 mg of recombinant protein of apparent homogeneity per liter of bacterial culture. As discussed earlier [31], treatment with thrombin protease significantly destabilized both constructs of Grb2 and rendered them proteolytically unstable, most likely due to their structural flexibility. For this reason, all experiments reported herein were carried out on recombinant fusion constructs of Grb2 and Grb2_ΔSH2, each containing a Trx-tag at the N-terminus and a His-tag at the C-terminus. The tags were found to have no effect on the binding of Grb2 to peptide ligands derived from Sos1 and Gab1. Protein concentrations were determined by both fluorescence using Invitrogen Quant-It assay and absorbance at 280 nm using extinction co-efficients of 52,160 M^{-1} cm^{-1} and 43,680 M^{-1} cm^{-1} for the recombinant full-length Grb2 and the truncated construct Grb2_ΔSH2. The extinction co-efficients were calculated from amino acid sequence alone using the online software ProtParam at ExPasy Server [32]. Results from both methods were in an excellent agreement.

Site-directed mutagenesis

pET102 bacterial expression vector expressing wildtype Grb2 (Grb2_WT) was subjected to Stratagene Quikchange II site-directed mutagenesis kit to generate D15G (Grb2_D15G), E171A (Grb2_E171A) and G173D (Grb2_G173D) mutants of full-length protein (Fig. 1b). All mutant constructs were expressed, purified and characterized as described above. When analyzed by size-exclusion chromatography (SEC) using Superdex 200 column, all mutant constructs exhibited virtually indistinguishable elution volumes to those observed for Grb2_WT, implying that the point substitution of specific residues did not lead to protein unfolding and that the mutant constructs retained the compact globular fold characteristic of wildtype protein. These observations were further confirmed by circular dichroism (CD) analysis.

Peptide synthesis

12-mer peptides spanning the binding site for the nSH3 and cSH3 domains of Grb2 within human Sos1 and the binding site for the cSH3 domain of Grb2 within human Gab1 were commercially obtained from GenScript Corporation. The peptide sequences are shown below:

- Sos1 peptide 1148-PVPPPVPPRRRP-1159,
- Gab1 peptide 516-PPPVDRNLKPDR-527,

The peptide concentrations were measured gravimetrically.

ITC analysis

Isothermal titration calorimetry (ITC) experiments were performed on a Microcal VP-ITC instrument and data were acquired and processed using fully automized features in Microcal ORIGIN software. Briefly, protein and peptide samples were prepared either in Tris buffer (50 mM Tris, 200 mM NaCl, 1 mM EDTA and 5 mM β-mercaptoethanol at pH 8.0) or phosphate buffer (50 mM sodium phosphate, 200 mM NaCl, 1 mM EDTA and 5 mM β-mercaptoethanol at pH 8.0). The experiments were initiated at 25 °C by injecting 25 × 10 μl aliquots of 2–4 mM of each peptide from the syringe into the calorimetric cell containing 1.8 ml of 50–200 μM of protein solution. Due to poor stability of Grb2 in phosphate buffer, Grb2 concentration in the calorimetric cell was closer to 50 μM for measurements conducted in Phosphate buffer, while measurements conducted in Tris buffer typically contained Grb2 over 100 μM in the calorimetric cell. For competition experiments, the competing peptide was pre-equilibrated with protein solution in the calorimetric cell at a protein-to-peptide molar ratio of 1:10 prior to injection of the other peptide from the syringe as described above. All other control experiments and data processing were performed as described earlier [28,29]. Briefly, the values for stoichiometry (n), affinity (K_d) and enthalpy (ΔH) of binding were obtained from the fit of a function, based on the binding of a ligand to a macromolecule [33], to the ITC isotherms assuming either one-site model or two-site model. In the case of data fitting to the two-site model, the stoichiometry (n) of binding was fixed at unity for each site to allow the convergence of other parameters (a limitation of fit of ITC data to two-site model). Free energy of binding (ΔG) was calculated from the relationship $\Delta G = RT\ln K_d$, where R is the universal molar gas constant (1.99 cal/mol/K) and T is the absolute temperature (K). Entropic contribution ($T\Delta S$) to binding was calculated from the relationship $T\Delta S = \Delta H - \Delta G$. Errors were calculated from 2 to 3 independent measurements. All errors are given to one standard deviation. It is of worthy note here that in order to ascertain greater confidence in the accuracy of thermodynamic parameters determined using ITC, it is desirable for measurements to be conducted under conditions where the experimental window of $5 < c < 500$ is met. The c-value is a dimensionless parameter defined as the ratio of protein concentration (μM) in the calorimetric cell to the equilibrium dissociation constant (μM) for the binding of an appropriate ligand or peptide. Put simply, the c-value constraint arises from the basic fact that the protein concentration in the calorimetric cell should be ideally between 5-fold and 500-fold higher than the equilibrium dissociation constant. However, for low-affinity systems, as the one under study here, it is not always possible to work in the experimental window of $5 < c < 500$ due to the requirement of rather large concentrations of both the protein and the ligand. Indeed, we employed virtually saturating concentrations for both Grb2 constructs and the peptides. The Grb2 constructs, particularly the mutant constructs, are extremely unstable in Phosphate buffer with concentrations barely reaching above 50 μM, while concentrations as high as 200 μM are surmountable in Tris buffer without causing protein aggregation. Even if it had been feasible to obtain wildtype Grb2 and various mutant constructs thereof at concentrations higher than 200 μM, the limiting solubility of Sos1 and Gab1 peptides in aqueous buffers would have posed additional technical hurdles. In light of such experimental limitations, our measurements were typically carried out in the experimental window of $1 < c < 5$. Nonetheless, a rather high accuracy of thermodynamic parameters reported herein can be expected due to the fulfillment of following conditions: (1) the ITC isotherms were obtained over a large titration window and allowed to reach near-saturation; (2) the concentrations of both the protein and the peptides were determined with high accuracy; (3) the signal-to-noise ratio was excellent and typically close to 100; and (4) the stoichiometries of binding were known to be either 1 or 2 for all experiments. Provided that the above conditions are met, a recent study indeed indicates that accurate thermodynamic parameters can be obtained for low-affinity systems in the experimental window of $1 < c < 5$ [34].

CD analysis

Circular dichroism (CD) measurements were conducted on a Bio-Logic MOS450 spectrometer equipped with a CD accessory and thermostatically controlled with a water bath at 25 °C. All data were acquired on a 50 μM of full-length wildtype Grb2 alone or pre-equilibrated with two molar-equivalents of either Sos1 peptide or Gab1 peptide or both peptides and processed using the Biokine software. Protein and peptide samples were prepared in 10 mM Sodium phosphate at pH 8.0 and analyzed using a quartz cuvette with either a 2-mm pathlength in the wavelength range 180–250 nm (far-UV) or 10-mm pathlength in the wavelength range 250–350 nm (near-UV). The contributions of Trx-tag and peptides to Grb2 ellipticity were removed by subtraction of appropriate control spectra obtained in a similar manner. Each data set represents an average of 4 scans acquired at 1 nm intervals. Data were recorded with a slit bandwidth of 2 nm at a scan rate of 3 nm/min. The observed ellipticity (ΔA) in mdeg was converted to molar ellipticity ($[\theta]$) as a function of wavelength (λ) of electromagnetic radiation using the equation: $[\theta] = (10^5 \Delta A/cl)$ deg cm^2 dmol^{-1}, where c is the protein concentration in μM and l is the cuvette pathlength in cm.

Macromolecular modeling

Macromolecular modeling (MM) was employed to construct 3D atomic models of full-length Grb2 in complex with Sos1 and Gab1 peptides using the MODELLER software based on homology modeling [35]. The structure of Grb2 in complex with Sos1 peptides bound to the nSH3 and cSH3 domains was modeled using the X-ray structure of Grb2 alone (1GRI) and the NMR structure of isolated nSH3 domain bound to Sos1 peptide (4GBQ) as templates. The structure of Grb2 in complex with Sos1 peptide bound to the nSH3 domain and Gab1 peptide bound to the cSH3 was modeled using the X-ray structure of Grb2 alone (1GRI), the NMR structure of isolated nSH3 domain bound to Sos1 peptide (4GBQ) and the X-ray structure of cSH3 domain of Grap2 bound to SLP76 peptide (1H3H) as templates. Additionally, hydrogen bonding restraints between specific pairs of residues involved in salt bridging were introduced in agreement with thermodynamic data reported previously [28,29]. It should be noted here that Grap2 is also constructed on the nSH3-SH2-cSH3 signaling module and shares high sequence identity with Grb2, while the SLP76 peptide contains the PXXXRXXKP motif found within Gab1 for binding to the cSH3 domain of Grb2. In each case, a total of 100 structural models were calculated and the structure with the lowest energy, as judged by the MODELLER Objective Function, was selected for further energy minimization in MODELLER prior to analysis. The structures were rendered using RIBBONS [36]. All other calculations were performed on the lowest energy structural model.

Results and discussion

Grb2 binds to both the Sos1 and Gab1 peptides with a 1:1 stoichiometry

A corollary of our hypothesis is that the cSH3 domain in the context of full-length Grb2 does not bind to Sos1 and thereby exclusively interacts with Gab1 in a non-competitive manner. To test that this is so, we measured the binding of full-length wildtype Grb2 (Grb2_WT) to peptides derived from Sos1 (PVPPPVPPRRRP) and Gab1 (PPPVDRNLKPDR). Fig. 2 shows representative ITC data

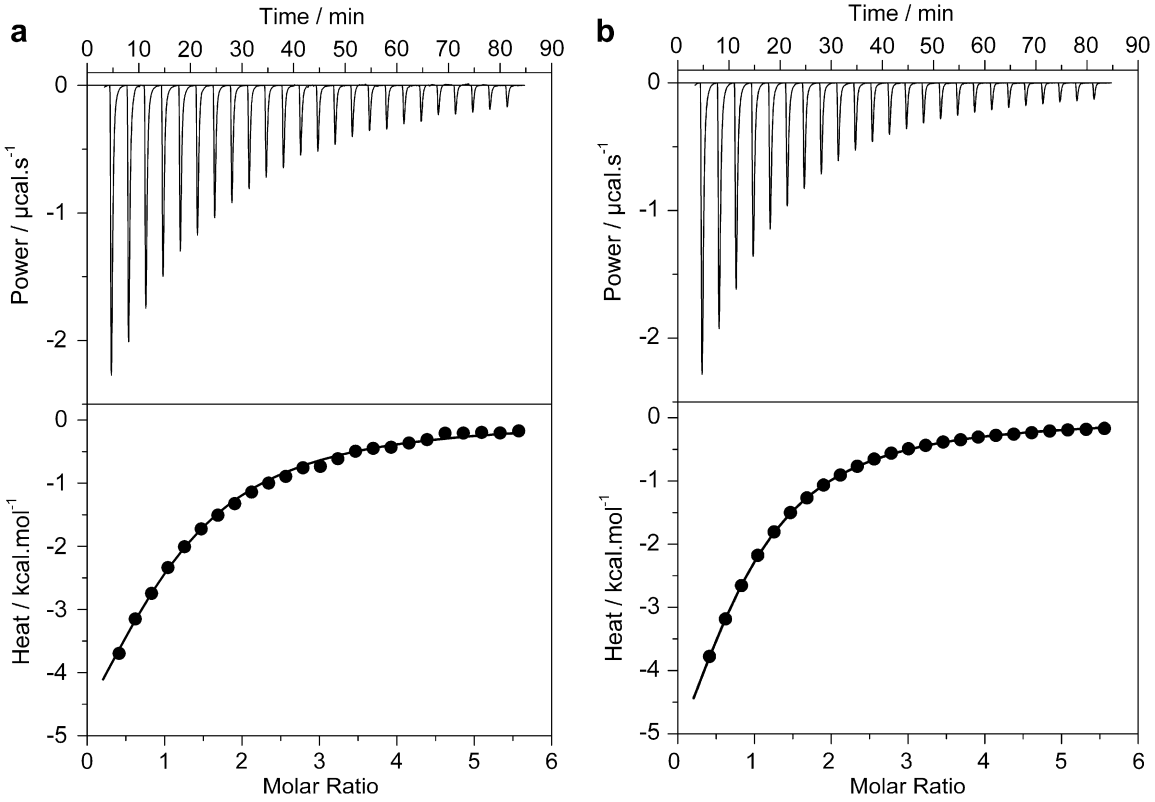

Fig. 2. Representative ITC isotherms obtained for the binding of Sos1 and Gab1 peptides to full-length wildtype Grb2 (Grb2_WT) in Tris buffer. (a) Binding of Sos1 peptide to Grb2_WT. (b) Binding of Gab1 peptide to Grb2_WT. The upper panels show the raw ITC data expressed as change in thermal power with respect to time over the period of titration. In the lower panels, change in molar heat is expressed as a function of peptide-to-protein molar ratio. The solid lines in the lower panels show the fit of data to a one-site model, based on the binding of a ligand to a macromolecule [33], as incorporated in the Microcal Origin software.

obtained from such measurements in Tris buffer. It should be noted here that the Sos1 peptide contains the PXψPXRRR consensus motif that has been shown to bind to both the nSH3 and cSH3 domains, while the Gab1 peptide conforms to the PXXXRXXK consensus motif known to exclusively interact with the cSH3 domain [14,25–29]. In light of these considerations, one would expect the binding of Sos1 and Gab1 peptides to full-length Grb2 with stoichiometries of 2:1 and 1:1, respectively. Our data however suggest that both the Sos1 and Gab1 peptides bind to Grb2_WT with a stoichiometry of 1:1 (Tables 1 and 2). Given that the formation of Sos1–Grb2–Gab1 ternary signaling complex proceeds in a non-competitive manner [30], the most straightforward interpretation of these salient observations is that the Sos1 peptide binds only to the nSH3 domain but not the cSH3 domain, while the Gab1 peptide binds only to the cSH3 domain in the context of full-length Grb2. To further investigate that Sos1 and Gab1 respectively bind to the nSH3 domain and the cSH3 domain in the context of full-length Grb2, we conducted competition experiments (Fig. 3). Pre-equilibration of Grb2 with Gab1 peptide, so as to block access to the cSH3 domain, had negligible effect on the energetics of binding of Sos1 peptide to Grb2 (Fig. 3a and Table 1). Similarly, pre-equilibration of Grb2 with Sos1 peptide, so as to block access to the nSH3 domain, had little effect on the energetics of binding of Gab1 peptide to Grb2 (Fig. 3b and Table 2). These key findings indicate that Sos1 and Gab1 peptides indeed respectively bind to the nSH3 and cSH3 domains in the context of full-length Grb2 and do so in a non-competitive manner. In an effort to further demonstrate their physiological significance so as to ensure that these observations are not dependent on buffer conditions, particularly in light of the rather high ionization enthalpy of Tris buffer, we also conducted ITC measurements in Phosphate buffer. As shown in Fig. 4, it is clearly evident that the stoichiometries and energetics of binding of Sos1 and Gab1 peptides to Grb2 in Tris buffer versus Phosphate buffer are virtually indistinguishable. It is also of worthy note that the binding of both the Sos1 and Gab1 peptides to Grb2 is largely driven by favorable enthalpic contribution accompanied by entropic penalty (Tables 1 and 2). Such an interplay between underlying thermodynamic forces suggests that electrostatic forces play a dominant role in driving these protein–protein interactions—an observation that is consistent with the knowledge that SH3-ligand interactions are largely under electrostatic control [37–40]. It is equally interesting to note that both the Sos1 and Gab1 peptides bind to Grb2 with very similar affinities and underlying thermodynamics despite their distinct modes of binding [25,26,41–45]. That this is so argues strongly that isostructures and isoenergetics may not necessarily correlate and urges a great deal of caution in a priori attempts to predict energetics of binding from structural information alone.

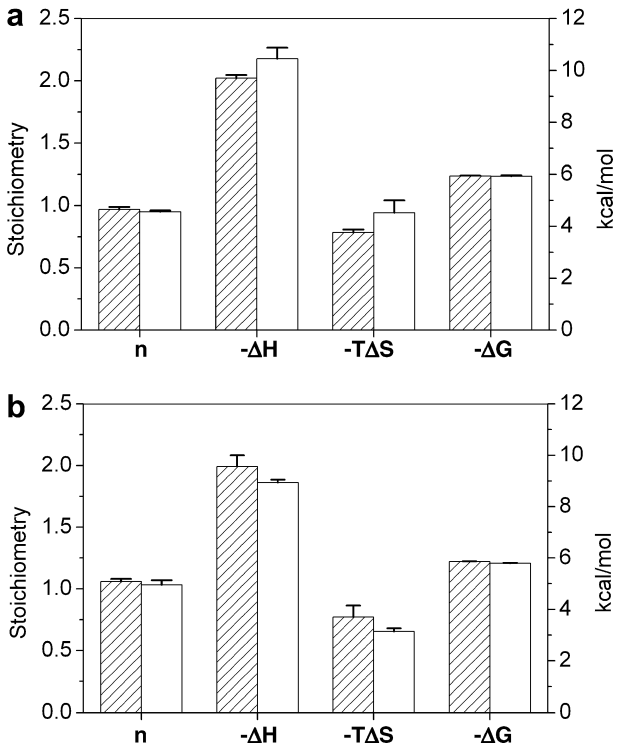

Fig. 3. Comparison of thermodynamic parameters n, ΔH, $T\Delta S$ and ΔG for the binding of Sos1 and Gab1 peptides to full-length wildtype Grb2 (Grb2_WT) under competitive and non-competitive settings in Tris buffer. (a) Binding of Sos1 peptide to Grb2_WT alone (shaded columns) and Grb2_WT pre-equilibrated with Gab1 peptide (unshaded columns). (b) Binding of Gab1 peptide to Grb2_WT alone (shaded columns) and Grb2_WT pre-equilibrated with Sos1 peptide (unshaded columns). All parameters were directly determined from ITC analysis.

Binding of Sos1 peptide to Grb2 induces allosteric inhibition of the cSH3 domain for subsequent loading of a second molecule of Sos1

To elucidate whether the cSH3 domain is auto-inhibited for binding to Sos1 in the context of full-length wildtype Grb2 (Grb2_WT) or whether the binding of Sos1 to the nSH3 domain

Table 1
Experimentally determined thermodynamic parameters obtained from ITC measurements for the binding of Sos1 peptide to various constructs of Grb2 alone and pre-equilibrated with Gab1 peptide in Tris buffer assuming one-site model.

	n	K_d (μM)	ΔH (kcal mol^{-1})	$T\Delta S$ (kcal mol^{-1})	ΔG (kcal mol^{-1})
Grb2_WT	0.97 ± 0.02	45.25 ± 0.58	−9.70 ± 0.12	−3.76 ± 0.12	−5.94 ± 0.01
Grb2_D15G	0.97 ± 0.06	129.06 ± 6.93	−7.50 ± 0.04	−2.19 ± 0.01	−5.31 ± 0.03
Grb2_E171A	1.04 ± 0.01	44.77 ± 0.69	−11.43 ± 0.18	−5.49 ± 0.19	−5.94 ± 0.02
Grb2_G173D	1.99 ± 0.08	42.55 ± 1.05	−6.25 ± 0.16	−0.31 ± 0.18	−5.97 ± 0.01
Grb2_ΔSH2	2.00 ± 0.04	83.68 ± 0.49	−6.55 ± 0.04	−0.98 ± 0.04	−5.57 ± 0.01
Grb2_WT + Gab1 peptide	0.95 ± 0.01	46.40 ± 3.03	−10.45 ± 0.43	−4.53 ± 0.47	−5.92 ± 0.04

Table 2
Experimentally determined thermodynamic parameters obtained from ITC measurements for the binding of Gab1 peptide to various constructs of Grb2 alone and pre-equilibrated with Sos1 peptide in Tris buffer assuming one-site model.

	n	K_d (μM)	ΔH (kcal mol^{-1})	$T\Delta S$ (kcal mol^{-1})	ΔG (kcal mol^{-1})
Grb2_WT	1.06 ± 0.02	51.03 ± 0.96	−9.56 ± 0.44	−3.70 ± 0.45	−5.86 ± 0.01
Grb2_ΔSH2	1.07 ± 0.01	50.26 ± 0.36	−9.75 ± 0.01	−3.88 ± 0.01	−5.87 ± 0.01
Grb2_WT + Sos1 peptide	1.03 ± 0.04	56.35 ± 1.12	−8.94 ± 0.11	−3.14 ± 0.12	−5.80 ± 0.01

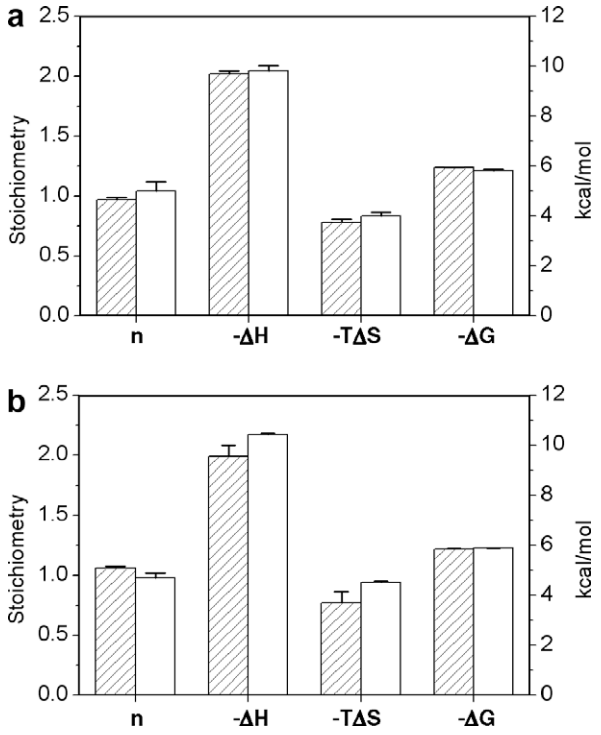

Fig. 4. Comparison of thermodynamic parameters n, ΔH, $T\Delta S$ and ΔG for the binding of Sos1 and Gab1 peptides to full-length wildtype Grb2 (Grb2_WT) under different buffer conditions. (a) Binding of Sos1 peptide to Grb2_WT in Tris buffer (shaded columns) and Phosphate buffer (unshaded columns). (b) Binding of Gab1 peptide to Grb2_WT in Tris buffer (shaded columns) and Phosphate buffer (unshaded columns). All parameters were directly determined from ITC analysis.

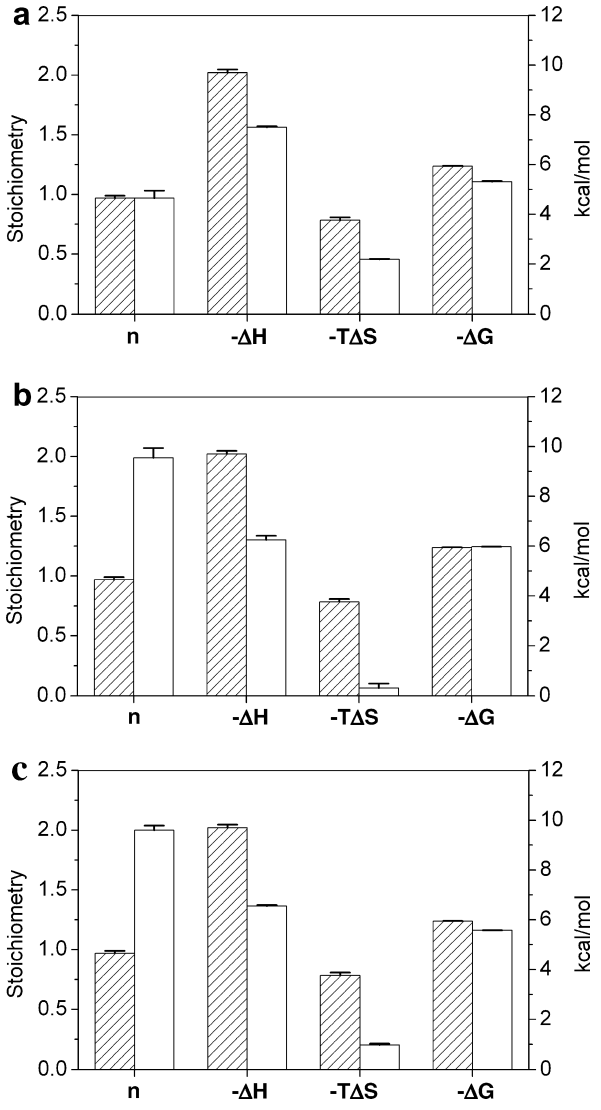

Fig. 5. Effect of various point and deletion mutations on the thermodynamic parameters n, ΔH, $T\Delta S$ and ΔG for the binding of Sos1 peptide to various constructs of Grb2 in Tris buffer. (a) Binding of Sos1 peptide to Grb2_WT (shaded columns) and Grb2_D15G (unshaded columns). (b) Binding of Sos1 peptide to Grb2_WT (shaded columns) and Grb2_G173D (unshaded columns). (c) Binding of Sos1 peptide to Grb2_WT (shaded columns) and Grb2_ΔSH2 (unshaded columns). All parameters were directly determined from ITC analysis.

is required for its inhibition, we measured the binding of Sos1 peptide to D15G mutant of full-length Grb2 (Grb2_D15G). Given that glycine substitution of D15 is sufficient to abrogate the binding of Sos1 to the nSH3 domain [28], the Grb2_D15G construct should provide a stern test of how the cSH3 domain behaves toward Sos1 in the context of full-length protein. As indicated in Fig. 5a and Table 1, Sos1 peptide binds to the cSH3 domain in the context of Grb2_D15G construct in a manner akin to its binding to nSH3 domain within the full-length Grb2, albeit with a 3-fold weaker affinity as reported previously for the binding of Sos1 peptide to the isolated cSH3 domain [28,29]. This salient observation implies that the preemptive binding of Sos1 to the nSH3 domain is obligatory for the allosteric inhibition of cSH3 domain for subsequent loading of a second molecule of Sos1. We also wondered whether the integrity of cSH3 domain for Sos1-binding is a pre-requisite for the binding of nSH3 domain to Sos1. To test this, we next measured the binding of Sos1 peptide to E171A mutant of full-length Grb2 (Grb2_E171A) in light of the knowledge that the substitution of E171 with alanine abrogates the binding of Sos1 to the cSH3 domain [28]. Our data suggest that the Sos1 peptide binds to Grb2_E171A construct with energetics that are similar to those observed for its binding to Grb2_WT (Table 1), implying that the integrity of cSH3 domain for Sos1-binding is not required for the binding of Sos1 to the nSH3 domain.

A subtle conformational change is sufficient to inhibit the binding of Sos1 to cSH3 domain within Grb2

In light of the knowledge that the G173D mutation of cSH3 domain renders it nSH3-mimetic [28,29], we also set out to investigate the extent to which Sos1-binding pocket within the cSH3 domain is sterically blocked upon the binding of Sos1 to the nSH3 domain. Our data suggest that the Sos1 peptide binds to the G173D mutant of full-length Grb2 (Grb2_G173D) with a stoichiometry of 2:1 (Fig. 5b and Table 1), implying that the Sos1-binding pocket within the cSH3 domain is only partially blocked so as to allow access to Gab1 but not Sos1. Because the Sos1 peptide appears to bind to both the nSH3 and cSH3 domains within the Grb2_G173D construct, we also analyzed the corresponding ITC data to a two-site model in lieu of the one-site model discussed above (Table 3). The fit of such data to a two-site model indeed generated underlying binding affinities and energetics similar to those observed for the isolated nSH3 domain and the G173D mutant of isolated cSH3 domain reported previously [28]. It should be noted here that the binding of Sos1 peptide to nSH3 and cSH3 domains employs distinct mechanisms as noted previously [29]. Thus, while only one intermolecular salt bridge is critical for the binding of Sos1 to the nSH3 domain, three are needed in the case of cSH3 domain. It is thus conceivable that only a slight re-orienta-

Table 3
Experimentally determined thermodynamic parameters obtained from ITC measurements for the binding of Sos1 peptide to Grb2_G173D and Grb2_ΔSH2 constructs in Tris buffer assuming two-site model.

	Site 1				Site 2			
	K_d (μM)	ΔH (kcal mol^{-1})	$T\Delta S$ (kcal mol^{-1})	ΔG (kcal mol^{-1})	K_d (μM)	ΔH (kcal mol^{-1})	$T\Delta S$ (kcal mol^{-1})	ΔG (kcal mol^{-1})
Grb2_G173D	40.23 ± 2.28	−8.49 ± 0.49	−2.48 ± 0.52	−6.00 ± 0.03	50.85 ± 2.92	−4.37 ± 0.97	+1.50 ± 0.93	−5.86 ± 0.03
Grb2_ΔSH2	40.26 ± 4.55	−8.91 ± 0.47	−2.90 ± 0.54	−6.00 ± 0.07	121.63 ± 5.43	−4.49 ± 0.22	+0.86 ± 0.25	−5.35 ± 0.03

tion of residues within the cSH3 domain involved in the formation of salt bridges with the incoming Sos1 peptide is sufficient to block its binding rather than a major structural re-arrangement of the binding groove. Taken together, these data imply that the binding of one molecule of Sos1 to the nSH3 domain somehow causes a subtle conformational change in Grb2 such that the binding of a second molecule of Sos1 to the cSH3 domain is somehow hindered yet allowing access to Gab1 in an allosteric manner.

SH2 domain mediates allosteric communication between the SH3 domains

To further explore the structural basis of allosteric inhibition of cSH3 domain toward Sos1 recognition, we also analyzed the binding of Sos1 peptide to a truncated construct of Grb2 in which the central SH2 domain was excised out and the two terminal SH3 domains were fused together via a flexible inter-domain loop (Grb2_ΔSH2). Our findings reveal that the Sos1 peptide binds to the Grb2_ΔSH2 construct with a stoichiometry of 2:1 (Fig. 5c), arguing strongly that the SH2 domain is critical for mediating allosteric communication between the nSH3 and cSH3 domains for their respective binding to Sos1 and Gab1 in a mutually inclusive manner. It is of worthy note that the binding affinity of Sos1 peptide to Grb2_ΔSH2 construct is intermediate between that observed for its binding to isolated nSH3 and cSH3 domains reported previously [28]. To deconvolute the binding of Sos1 peptide to the nSH3 and cSH3 domains within the Grb2_ΔSH2 construct, we also analyzed the corresponding ITC data to a two-site model in lieu of the one-site model discussed above (Table 3). As expected, the fit of such data to a two-site model generated underlying binding affinities and energetics similar to those observed for the isolated nSH3 domain and cSH3 domains [28]. As a control, Gab1 peptide bound to Grb2_ΔSH2 construct with energetics that are virtually indistinguishable from those observed for its binding to Grb2_WT construct (Table 1), supporting the view that the cSH3 domain behaves similarly in both constructs. 3D atomic structure of Grb2 reveals that the two SH3 domains are juxtaposed close to each other in the context of the full-length protein and that the SH2 domain likely plays a key role in orienting the two SH3 domains relative to each other [46]. It is thus conceivable that the SH2 domain merely serves as a scaffold in bringing the two SH3 domains together and thereby allowing them to engage in allosteric communication solely through space. On the other hand, the possibility that the allosteric communication between the two SH3 domains is directly transmitted through the SH2 domain cannot be excluded. 3D structures of Grb2_WT and Grb2_ΔSH2 constructs alone and in complex with Sos1 and Gab1 peptides would clearly provide invaluable insights into the detailed structural basis of allosteric communication observed here between the two SH3 domains.

Binding of Sos1 and Gab1 induces subtle secondary and tertiary structural changes within Grb2

In an effort to directly assess the extent to which the binding of Sos1 to nSH3 domain may be coupled to structural changes within Grb2 such that the cSH3 domain can no longer accommodate a second molecule of Sos1 but yet remains conducive to the binding of Gab1, we conducted CD analysis of Grb2 alone and in complex with appropriate peptides (Fig. 6). Expectedly, the far-UV spectrum of Grb2 displays features characteristic of mixed αβ proteins with maxima centered around 190 nm and 210 nm flanked by minima centered around 200 nm and 220 nm, respectively (Fig. 6a). It is noteworthy that while the far-UV spectrum of Grb2 exhibits global changes upon the addition of Sos1 and Gab1 peptides alone or in combination, these are particularly pronounced around the 190-nm band. These salient observations suggest that the binding of both Sos1 and Gab1 peptides induces secondary structural changes within Grb2 and that they most likely arise from the formation of hydrophobic grooves within the SH3 β-barrels for accommodating the respective peptides upon their binding. Interestingly, such secondary structural changes are exquisitely mirrored by tertiary structural changes within Grb2 as evidenced in the near-UV spectra upon the addition of Sos1 and Gab1 peptides alone or in combination (Fig. 6b). In particular, it should be noted that the addition of peptides alone or in combination results in substantial enhancement of the bands around 255 nm and 280 nm, implying the formation of local tertiary structure around the triplet of aromatic residues F9/W36/Y52 and F167/W193/Y209 lining the binding grooves in nSH3 and cSH3 domains [28], respectively. Although these CD measurements are of highly qualitative nature and thus do not provide the physical basis of how the binding of Sos1 to the nSH3 domain may trigger a conformational change within Grb2 such that the cSH3 domain is only accessible to Gab1, the fact that Grb2 appears to be a highly flexible molecule by virtue of its ability to undergo discernable secondary and tertiary structural changes upon binding to Sos1 and Gab1 peptides nonetheless supports the notion that allostery is likely to play a central role in mediating communication between the nSH3 and cSH3 domains so as to allow the assembly of Sos1–Grb2–Gab1 ternary signaling complex in a non-competitive manner.

3D atomic model of Sos1–Grb2–Gab1 ternary signaling complex provides key insights into the structural basis of allosteric regulation

Although efforts by others and us directed at the determination of X-ray or NMR structures of full-length Grb2 bound to Sos1 or Gab1 constructs of any sort over the past decade or so have met no success, presumably due to the transient nature of Sos1–Grb2–Gab1 complex, we have nonetheless made an attempt here to create a crude 3D structural model of how the binding of one molecule of Sos1 to the nSH3 domain may allosterically induce a conformational change within Grb2 such that the loading of a second molecule of Sos1 onto the cSH3 domain is blocked and, in so doing, allowing Gab1 access to the cSH3 domain in an exclusively non-competitive manner to generate the Sos1–Grb2–Gab1 ternary complex (Fig. 7). Our structural model indicates that the binding of Sos1 peptide to nSH3 and cSH3 domains employs distinct mechanisms and that such differential behavior of Sos1 towards its putative SH3 targets within Grb2 may account for its ability to selectively prefer one over the other (Fig. 7a). It is noteworthy that while the binding of Sos1 peptide to the nSH3

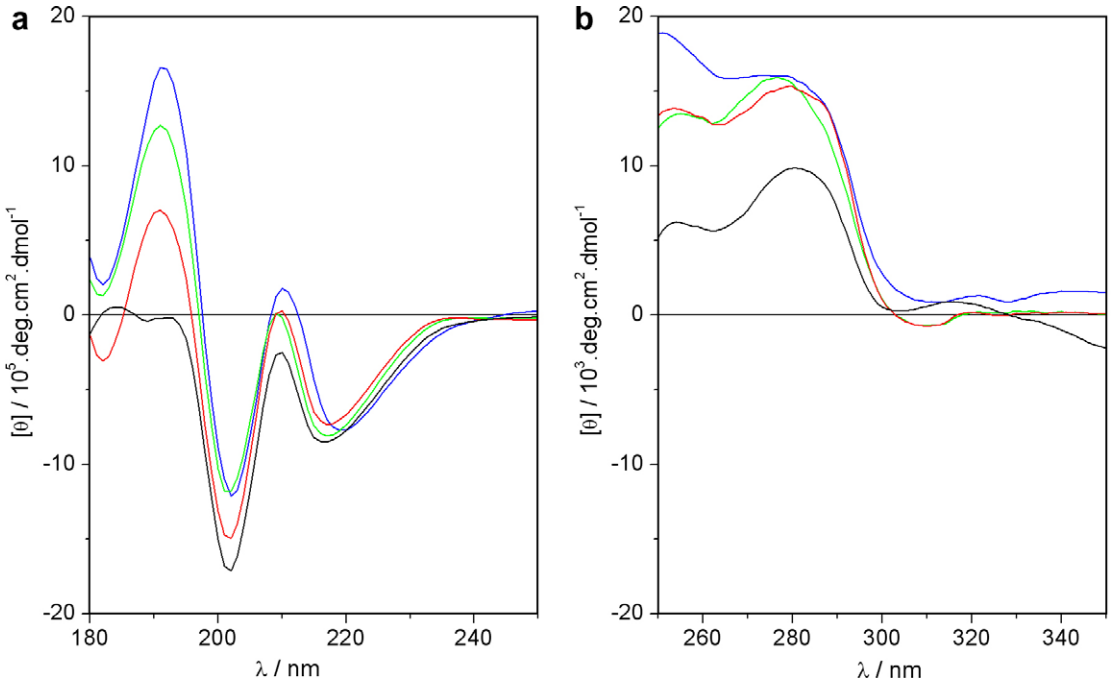

Fig. 6. Representative CD spectra of full-length wildtype Grb2 alone and in complex with Sos1 and Gab1 peptides (with the contributions from the Trx-tag and peptides removed). (a) Far-UV spectra of Grb2 alone (black), Grb2 bound to Sos1 peptide (red), Grb2 bound to Gab1 peptide (green) and, Grb2 bound to both Sos1 and Gab1 peptides (blue). (b) Near-UV spectra of Grb2 alone (black), Grb2 bound to Sos1 peptide (red), Grb2 bound to Gab1 peptide (green) and, Grb2 bound to both Sos1 and Gab1 peptides (blue). Note that all spectra are expressed in terms of molar ellipticity ([θ]) as a function of wavelength (λ) of electromagnetic radiation. (For interpretation of the references to color in this figure legend, the reader is referred to the web version of this paper.)

domain requires a narrow groove running parallel to the RT loop, it occupies a much wider groove in the cSH3 domain that stretches from the RT loop on one side of the β-barrel fold to the n-Src loop on the other side. Such differences largely arise from the requirement of one or more intermolecular salt bridges. Thus, while the binding of Sos1 peptide to the nSH3 domain only strictly requires one such salt bridge formed by the R1156-D15 ion pair, the formation of three such salt bridges through the engagement of the R1156-E171, R1157-D187 and R1158-D190 ion pairs is mandatory for the binding of Sos1 peptide to the cSH3 domain as reported previously [28,29]. It is plausible to envision a scenario whereby the binding of Sos1 to the nSH3 domain somehow allosterically induces a conformational change within Grb2 such that one or more of the three acidic residues within the cSH3 domain involved in the formation of intermolecular salt bridges become misaligned and the resulting orientation of these critical residues can no longer accommodate Sos1 but yet retains the integrity to recognize Gab1. The binding mode of Gab1 to the cSH3 domain is indeed distinct from that of Sos1 (Fig. 7b). Unlike the requirement of three acidic residues within the cSH3 binding groove to participate in the formation of intermolecular ion pairs with Sos1, only E171 appears to be necessary for binding to Gab1 peptide. Additionally, unlike the Sos1 peptide that adapts a relatively open left-handed polyproline type II (PPII) helical conformation, the Gab1 peptide adapts a much tighter 3_{10}-helical conformation upon binding to the cSH3 domain. In particular, the 3_{10}-helical turn allows both R521 and K524 within the Gab1 consensus motif PXXXRXXKP to ion pair with E171 forming a tripartite salt bridge and thereby enabling Gab1 peptide to require a much narrower groove for binding to the cSH3 domain in a manner akin to the binding of Sos1 peptide to the nSH3 domain but in a remarkable contrast to the requirement of a much wider binding groove within the cSH3 domain for accommodating the Sos1 peptide. Because of such differences in the binding modes of Sos1 and Gab1 to the cSH3 domain, the binding of Sos1 to the nSH3 domain may only require subtle conformational changes within Grb2 to block the binding of a second molecule of Sos1 to the cSH3 domain and thereby handing it an exclusive right to bind to Gab1. It should also be noted here that the binding of Sos1 to the cSH3 domain in the context of full-length Grb2 is rescued by the introduction of G173D mutation located within the binding groove of cSH3 domain and exquisitely positioned and optimally aligned right next to E171 (Fig. 5b and Table 1). In light of the 3D structural models presented above (Fig. 7), the binding of Sos1 to the cSH3 domain within the Grb2_G173D construct could be envisioned through the ion pairing of R1156 with both the E171 and G173D so as to form a tripartite salt bridge in lieu of a mere R1156-E171 ion pair attainable in the context of wildtype Grb2. Consequently, the availability of additional free energy released upon the formation of an E171-R1156-G173D tripartite salt bridge in the context of Grb2_G173D construct may compensate for the loss of free energy resulting from the lack of formation of the other two ion pairs, namely R1157-D187 and R1158-D190, that are mandatory for the binding of Sos1 peptide to the cSH3 domain within wildtype Grb2. In other words, the binding of Sos1 to the cSH3 domain within Grb2_G173D construct may employ a distinct mechanism from that observed for the binding of Sos1 to the cSH3 domain within wildtype Grb2. Thus, while the binding of Sos1 to cSH3 domain within the wildtype Grb2 requires the formation of three ion pairs, namely R1156-E171, R1157-D187 and R1158-D190, formation of only the E171-R1156-G173D tripartite salt bridge may be necessary for the binding of Sos1 to the cSH3 domain within the Grb2_G173D construct. Such scenario involving the binding of Sos1 to the cSH3 domain within Grb2_G173D construct would by-pass the need for the optimal orientation and availability of acidic residues D187 and D190—the very factors that could account for the inability of Sos1 to bind to the cSH3 domain within wildtype Grb2. Taken together, the

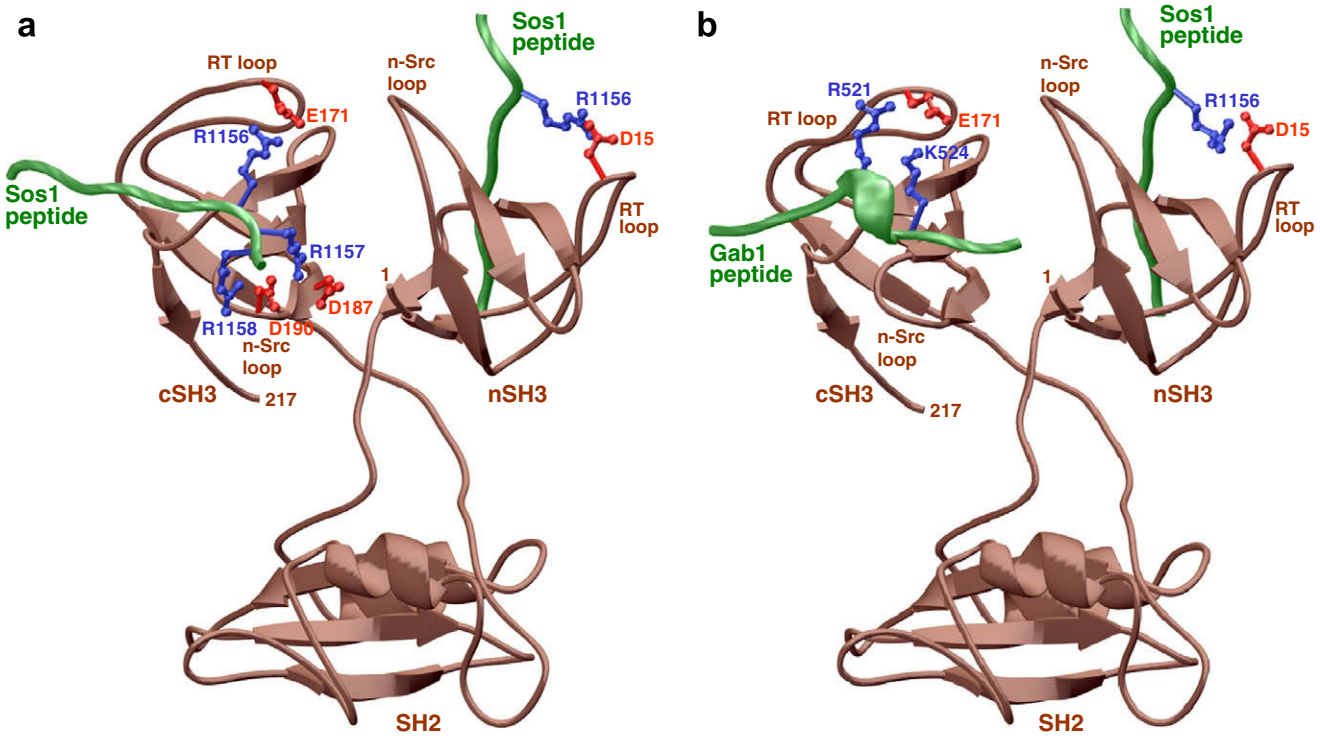

Fig. 7. 3D structural models of full-length Grb2 in complex with Sos1 and Gab1 peptides obtained using the MODELLER software based on homology modeling [35]. (a) Sos1 peptides bound to both nSH3 and cSH3 domains within Grb2. (b) Sos1 peptide bound to the nSH3 domain and Gab1 peptide bound to the cSH3 domain within Grb2. The backbone of Grb2 is depicted in brown, while the backbones of Sos1 and Gab1 peptides are shown in green. The sidechain atoms of residues within Grb2 and the peptides involved in intermolecular interaction are colored red and blue, respectively. (For interpretation of the references to color in this figure legend, the reader is referred to the web version of this paper.)

foregoing argument further corroborates the notion that a subtle conformational change within the cSH3 domain would suffice to inhibit its binding to Sos1 in the context of full-length wildtype Grb2.

Conclusions

Allostery is central to driving protein–ligand interactions in biological systems. The question is not whether proteins employ allostery in communicating with each other but rather under what context. The law of mass action embodies the notion that the assembly of a complex is accelerated with increasing concentrations of the two or more constituent components. In this context, allostery is thus a natural product of the need for proteins to interact to generate a biological effect in harmony with the laws of physics. Accumulating evidence from various systems studied over the past half century or so suggests that, although poorly understood and under-appreciated, allostery is the key to unlocking the secrets of many biological phenomena. Notable examples of allostery include the changes in protein structure upon covalent modifications such as phosphorylation [47–55], the binding of various transcription factors to DNA [56–60], the activation of proteins upon ligand binding [61–64] and, of course, the uptake of oxygen by hemoglobin [65]. Herein, we have provided compelling evidence that the binding of Sos1 and Gab1 to Grb2 in a non-competitive manner to generate the Sos1–Grb2–Gab1 ternary signaling complex employs an allosteric mechanism. While we have relied here on short peptides to mimic Sos1 and Gab1, due largely to inherent difficulties associated with isolation and purification of full-length Sos1 and Gab1 proteins, it should be noted that these peptides suffice par excellence for studying the binding of Sos1 and Gab1 to Grb2 using biophysical methods. Numerous X-ray and NMR structures of SH3 domains of Grb2 in complex with the peptides derived from Sos1 and Gab1 indeed support the notion that the critical residues within these proteins involved in the recognition of SH3 domains exclusively reside within the corresponding peptides employed here [25,26,41,42,45]. Despite such limitations, our study unequivocally demonstrates that Sos1 binds to the nSH3 domain in an allosteric manner so as to block the loading of a second molecule of Sos1 onto the cSH3 domain and thus enabling it to exclusively interact with Gab1. Fascinating as it may seem, our study however falls short of providing the physical basis of such allostery despite our continuing efforts to obtain suitable crystals of Sos1–Grb2–Gab1 ternary complex for structural analysis at atomic level. We believe that this may be due to the dynamic nature of Sos1–Grb2–Gab1 complex as a result of the rather weak equilibrium constants in the tens of micromolar range driving the assembly of constituent components. Such a scenario would be seemingly desirable under physiological context where the reversible nature of cellular signaling cascades demands the rapid reversibility of signaling complexes. However, the rather weak nature of Sos1–Grb2–Gab1 complex signals a poor outcome from a crystallographic standpoint. Nonetheless, our 3D atomic model of Sos1–Grb2–Gab1 ternary complex lends interesting insights into how a subtle conformational change within Grb2 upon the binding of Sos1 to the nSH3 domain may allow the cSH3 domain to exclusively interact with Gab1 in lieu of a second molecule of Sos1. In short, our study provides mechanistic insights into the assembly of a key signaling complex and profoundly argues for a greater role of allostery in cellular signaling cascades central to health and disease.

Acknowledgments

This work was supported by funds from the National Institutes of Health (Grant# R01-GM083897), the American Heart

Association (Grant# 0655087B) and the USylvester Braman Family Breast Cancer Institute to AF. CBM is a recipient of a post-doctoral fellowship from the National Institutes of Health (Award# T32-CA119929). BJD and AF are members of the Sheila and David Fuente Graduate Program in Cancer Biology at the Sylvester Comprehensive Cancer Center of the University of Miami. The authors are deeply indebted to Marius Sudol and Vineet Gupta for their critical reading of the manuscript and many helpful suggestions.

References

[1] J.C. Kendrew, G. Bodo, H.M. Dintzis, R.G. Parrish, H. Wyckoff, D.C. Phillips, Nature 181 (1958) 662–666.
[2] J. Monod, J.P. Changeux, F. Jacob, J. Mol. Biol. 6 (1963) 306–329.
[3] J. Monod, J. Wyman, J.P. Changeux, J. Mol. Biol. 12 (1965) 88–118.
[4] J. Kuriyan, D. Eisenberg, Nature 450 (2007) 983–990.
[5] P. Chardin, D. Cussac, S. Maignan, A. Ducruix, FEBS Lett. 369 (1995) 47–51.
[6] A. Nimnual, D. Bar-Sagi, Sci. STKE 2002 (2002) PE36.
[7] N. Li, A. Batzer, R. Daly, V. Yajnik, E. Skolnik, P. Chardin, D. Bar-Sagi, B. Margolis, J. Schlessinger, Nature 363 (1993) 85–88.
[8] N.W. Gale, S. Kaplan, E.J. Lowenstein, J. Schlessinger, D. Bar-Sagi, Nature 363 (1993) 88–92.
[9] M. Rozakis-Adcock, J. McGlade, G. Mbamalu, G. Pelicci, R. Daly, W. Li, A. Batzer, S. Thoma, J. Brugge, P.G. Pelicci, J. Schlessinger, T. Pawson, Nature 360 (1992) 689–692.
[10] E.J. Lowenstein, R.J. Daly, A.G. Batzer, W. Li, B. Margolis, R. Lammers, A. Ullrich, E.Y. Skolnik, D. Bar-Sagi, J. Schlessinger, Cell 70 (1992) 431–442.
[11] M. Rozakis-Adcock, R. Fernley, J. Wade, T. Pawson, D. Bowtell, Nature 363 (1993) 83–85.
[12] P. Chardin, J.H. Camonis, N.W. Gale, L. van Aelst, J. Schlessinger, M.H. Wigler, D. Bar-Sagi, Science 260 (1993) 1338–1343.
[13] U. Schaeper, N.H. Gehring, K.P. Fuchs, M. Sachs, B. Kempkes, W. Birchmeier, J. Cell. Biol. 149 (2000) 1419–1432.
[14] M. Lewitzky, C. Kardinal, N.H. Gehring, E.K. Schmidt, B. Konkol, M. Eulitz, W. Birchmeier, U. Schaeper, S.M. Feller, Oncogene 20 (2001) 1052–1062.
[15] K. Seedorf, G. Kostka, R. Lammers, P. Bashkin, R. Daly, W.H. Burgess, A.M. van der Bliek, J. Schlessinger, A. Ullrich, J. Biol. Chem. 269 (1994) 16009–16014.
[16] M. Vidal, J.L. Montiel, D. Cussac, F. Cornille, M. Duchesne, F. Parker, B. Tocque, B.P. Roques, C. Garbay, J. Biol. Chem. 273 (1998) 5343–5348.
[17] H. Odai, K. Sasaki, A. Iwamatsu, Y. Hanazono, T. Tanaka, K. Mitani, Y. Yazaki, H. Hirai, J. Biol. Chem. 270 (1995) 10800–10805.
[18] R.K. Park, W.T. Kyono, Y. Liu, D.L. Durden, J. Immunol. 160 (1998) 5018–5027.
[19] S.J. Moeller, E.D. Head, R.J. Sheaff, Mol. Cell. Biol. 23 (2003) 3735–3752.
[20] M.J. Robinson, M.H. Cobb, Curr. Opin. Cell Biol. 9 (1997) 180–186.
[21] J.M. Cunnick, S. Meng, Y. Ren, C. Desponts, H.G. Wang, J.Y. Djeu, J. Wu, J. Biol. Chem. 277 (2002) 9498–9504.
[22] H. Gu, B.G. Neel, Trends Cell Biol. 13 (2003) 122–130.
[23] T. Araki, H. Nawa, B.G. Neel, J. Biol. Chem. 278 (2003) 41677–41684.
[24] D. Kim, J. Chung, J. Biochem. Mol. Biol. 35 (2002) 106–115.
[25] M. Wittekind, C. Mapelli, V. Lee, V. Goldfarb, M.S. Friedrichs, C.A. Meyers, L. Mueller, J. Mol. Biol. 267 (1997) 933–952.
[26] M. Wittekind, C. Mapelli, B.T. Farmer 2nd, K.L. Suen, V. Goldfarb, J. Tsao, T. Lavoie, M. Barbacid, C.A. Meyers, L. Mueller, Biochemistry 33 (1994) 13531–13539.
[27] D. Kohda, H. Terasawa, S. Ichikawa, K. Ogura, H. Hatanaka, V. Mandiyan, A. Ullrich, J. Schlessinger, F. Inagaki, Structure 2 (1994) 1029–1040.
[28] C.B. McDonald, K.L. Seldeen, B.J. Deegan, A. Farooq, Arch. Biochem. Biophys. 479 (2008) 52–62.
[29] C.B. McDonald, K.L. Seldeen, B.J. Deegan, A. Farooq, Biochemistry 48 (2009) 4074–4085.
[30] S.H. Ong, Y.R. Hadari, N. Gotoh, G.R. Guy, J. Schlessinger, I. Lax, Proc. Natl. Acad. Sci. USA 98 (2001) 6074–6079.
[31] C.B. McDonald, K.L. Seldeen, B.J. Deegan, M.S. Lewis, A. Farooq, Arch. Biochem. Biophys. 475 (2008) 25–35.
[32] E. Gasteiger, C. Hoogland, A. Gattiker, S. Duvaud, M.R. Wilkins, R.D. Appel, A. Bairoch, in: J.M. Walker (Ed.), The Proteomics Protocols Handbook, Humana Press, Totowa, New Jersey, USA, 2005, pp. 571–607.
[33] T. Wiseman, S. Williston, J.F. Brandts, L.N. Lin, Anal. Biochem. 179 (1989) 131–137.
[34] W.B. Turnbull, A.H. Daranas, J. Am. Chem. Soc. 125 (2003) 14859–14866.
[35] M.A. Marti-Renom, A.C. Stuart, A. Fiser, R. Sanchez, F. Melo, A. Sali, Annu. Rev. Biophys. Biomol. Struct. 29 (2000) 291–325.
[36] M. Carson, J. Appl. Crystallogr. 24 (1991) 958–961.
[37] W.A. Lim, F.M. Richards, R.O. Fox, Nature 372 (1994) 375–379.
[38] H. Yu, J.K. Chen, S. Feng, D.C. Dalgarno, A.W. Brauer, S.L. Schreiber, Cell 76 (1994) 933–945.
[39] A.B. Sparks, J.E. Rider, N.G. Hoffman, D.M. Fowlkes, L.A. Quillam, B.K. Kay, Proc. Natl. Acad. Sci. USA 93 (1996) 1540–1544.
[40] G. Cesareni, S. Panni, G. Nardelli, L. Castagnoli, FEBS Lett. 513 (2002) 38–44.
[41] N. Goudreau, F. Cornille, M. Duchesne, F. Parker, B. Tocque, C. Garbay, B.P. Roques, Nat. Struct. Biol. 1 (1994) 898–907.
[42] H. Terasawa, D. Kohda, H. Hatanaka, S. Tsuchiya, K. Ogura, K. Nagata, S. Ishii, V. Mandiyan, A. Ullrich, J. Schlessinger, et al., Nat. Struct. Biol. 1 (1994) 891–897.
[43] M. Harkiolaki, M. Lewitzky, R.J. Gilbert, E.Y. Jones, R.P. Bourette, G. Mouchiroud, H. Sondermann, I. Moarefi, S.M. Feller, EMBO J. 22 (2003) 2571–2582.
[44] Q. Liu, D. Berry, P. Nash, T. Pawson, C.J. McGlade, S.S. Li, Mol. Cell 11 (2003) 471–481.
[45] M. Harkiolaki, T. Tsirka, M. Lewitzky, P.C. Simister, D. Joshi, L.E. Bird, E.Y. Jones, N. O'Reilly, S.M. Feller, Structure 17 (2009) 809–822.
[46] S. Maignan, J.P. Guilloteau, N. Fromage, B. Arnoux, J. Becquart, A. Ducruix, Science 268 (1995) 291–293.
[47] D. Barford, L.N. Johnson, Nature 340 (1989) 609–616.
[48] P. Hof, S. Pluskey, S. Dhe-Paganon, M.J. Eck, S.E. Shoelson, Cell 92 (1998) 441–450.
[49] B. Nagar, O. Hantschel, M.A. Young, K. Scheffzek, D. Veach, W. Bornmann, B. Clarkson, G. Superti-Furga, J. Kuriyan, Cell 112 (2003) 859–871.
[50] F. Sicheri, I. Moarefi, J. Kuriyan, Nature 385 (1997) 602–609.
[51] F. Sicheri, J. Kuriyan, Curr. Opin. Struct. Biol. 7 (1997) 777–785.
[52] W. Xu, S.C. Harrison, M.J. Eck, Nature 385 (1997) 595–602.
[53] S. Deindl, T.A. Kadlecek, T. Brdicka, X. Cao, A. Weiss, J. Kuriyan, Cell 129 (2007) 735–746.
[54] D. Lietha, X. Cai, D.F. Ceccarelli, Y. Li, M.D. Schaller, M.J. Eck, Cell 129 (2007) 1177–1187.
[55] X. Zhang, J. Gureasko, K. Shen, P.A. Cole, J. Kuriyan, Cell 125 (2006) 1137–1149.
[56] C.O. Pabo, R.T. Sauer, Annu. Rev. Biochem. 61 (1992) 1053–1095.
[57] D.S. Wilson, B. Guenther, C. Desplan, J. Kuriyan, Cell 82 (1995) 709–719.
[58] T. Li, M.R. Stark, A.D. Johnson, C. Wolberger, Science 270 (1995) 262–269.
[59] E.M. Jacobson, P. Li, A. Leon-del-Rio, M.G. Rosenfeld, A.K. Aggarwal, Genes Dev. 11 (1997) 198–212.
[60] D.E. Piper, A.H. Batchelor, C.P. Chang, M.L. Cleary, C. Wolberger, Cell 96 (1999) 587–597.
[61] A.S. Kim, L.T. Kakalis, N. Abdul-Manan, G.A. Liu, M.K. Rosen, Nature 404 (2000) 151–158.
[62] A.I. Shulman, C. Larson, D.J. Mangelsdorf, R. Ranganathan, Cell 116 (2004) 417–429.
[63] A. Farooq, G. Chaturvedi, S. Mujtaba, O. Plotnikova, L. Zeng, C. Dhalluin, R. Ashton, M.-M. Zhou, Mol. Cell 7 (2001) 387–399.
[64] A. Farooq, L. Zeng, K.S. Yan, K.S. Ravichandran, M.-M. Zhou, Structure 11 (2003) 905–913.
[65] W.E. Royer Jr., H. Zhu, T.A. Gorr, J.F. Flores, J.E. Knapp, J. Biol. Chem. 280 (2005) 27477–27480.